Chemical Fluid Deposition of Pt−Based Bimetallic Nanoparticles on Multiwalled Carbon Nanotubes for Direct Methanol Fuel Cell Application

ARTICLE *in* ENERGY & FUELS · MAY 2007

Impact Factor: 2.79 · DOI: 10.1021/ef0606409

6 AUTHORS, INCLUDING:

Kenichi Shimizu
University of Oxford
17 PUBLICATIONS **310** CITATIONS
SEE PROFILE

Ying-Ying Lin
Texas A&M University
11 PUBLICATIONS **612** CITATIONS
SEE PROFILE

I. Francis Cheng
University of Idaho
83 PUBLICATIONS **1,798** CITATIONS
SEE PROFILE

Chemical Fluid Deposition of Pt-Based Bimetallic Nanoparticles on Multiwalled Carbon Nanotubes for Direct Methanol Fuel Cell Application

Clive H. Yen,[†] Kenichi Shimizu,[†] Ying-Ying Lin,[†] Franklin Bailey,[‡] I. Francis Cheng,[†] and Chien M. Wai*,[†]

Department of Chemistry, and Electron Microscopy Center, University of Idaho, Moscow, Idaho 83844

Received December 14, 2006. Revised Manuscript Received April 20, 2007

A simple and green method of depositing platinum-based bimetallic nanoparticles (Pt−Ru, Pt−Cu, Pt−Au, Pt−Pd, and Pt−Ni) on multiwalled carbon nanotubes (MWCNTs) in supercritical fluid carbon dioxide (sc-CO_2) is described. CO_2-soluble metal precursors, such as metal acetylacetonates or hexafluoroacetylacetonates, were used in the experiments. Suitable temperature and pressure conditions for synthesizing each kind of bimetallic nanoparticle are studied. Characterizations of these nanocomposites, performed by transmission electron microscopy (TEM), energy-dispersive X-ray spectroscopy (EDS), and X-ray diffraction (XRD), all confirmed their presence. These MWCNT-supported bimetallic nanoparticles have average sizes varying from 2.8 to 9.3 nm. The application of these nanocomposites is demonstrated by using them as electrocatalysts for direct methanol fuel cell (DMFC). Their electrochemical activities are studied by using cyclic voltammetry (CV), and their efficiency to oxidize methanol to carbon dioxide is at least 60% better than the MWCNT-supported monometallic Pt nanoparticle catalyst reported previously.

1. Introduction

In recent years, studies of bimetallic nanoparticles as catalysts have drawn great interest because they often create synergistic effects that can improve catalytic activities of electrochemical reactions. Bimetallic nanoparticle catalysts usually include a primary metal that has a high performance in catalytic activity and a secondary metal that can help improve the catalytic activity or prevent poisoning problems. The advantages of using bimetallic nanoparticles for electrochemical reactions are known in the literature.[1−3] Most of the literature reports regarding bimetallic electrocatalysts are related to Pt−Ru, while combinations of Pt with other metals have also been reported.

Because bimetallic nanoparticles are extremely active, preventing their aggregation in electrochemical processes, such as in proton exchange membrane fuel cell (PEMFC) applications, is a problem that must be addressed for their commercial use. Recent reports show that multiwalled carbon nanotubes (MWCNTs) provide good supports for catalytic metal nanoparticles.[4,5] MWCNTs, which are known to conduct current and provide a high surface area for attachment of nanoparticles, are highly attractive for PEMFC applications.

In this paper, we use MWCNT as the support for deposition of bimetallic nanoparticles in supercritical fluid carbon dioxide (sc-CO_2). The advantages of using sc-CO_2 as a medium for nanoparticle synthesis and deposition are known in the literature.[6−8] Methods of preparing bimetallic nanoparticles in sc-CO_2 have been reported previously. Dhepe et al. reported a multistep impregnation with sc-CO_2 treatment for making Rh−Pt nanoparticles.[9] Another report by Kameo et al. used a fluorinated surfactant for making Ag−Pd nanoparticles.[10] Recently, Wakayama et al. synthesized Pt−Ru nanoporous fibers by a process called nanoscale casting under supercritical fluid (NC-SCF).[11] The chemical fluid deposition method (CFD) described in this paper is much simpler. It contains only a single hydrogen reduction/deposition step, and the reaction is rapid and clean. The main requirement of our deposition process is to have a couple of CO_2-soluble metal precursors (such as metal-β-diketonates) dissolved in the fluid phase. Hydrogen that is miscible with CO_2 is used as the reducing agent for metal reduction. This technique is also considered "green" because it reduces the amount of liquid or organic waste that is often produced during chemical reactions. In previous studies, we have demonstrated that Pt and Pt−Ru bimetallic nanoparticles prepared by this method are very effective electrocatalysts for anodic oxidation of

* To whom correspondence should be addressed. E-mail: cwai@uidaho.edu.
[†] Department of Chemistry.
[‡] Electron Microscopy Center.

(1) Chan, K.-Y.; Ding, J.; Ren, J.; Cheng, S.; Tsang, K. Y. *J. Mater. Chem.* **2004**, *14*, 505−516.
(2) Casado-Rivera, E.; Volpe, D. J.; Alden, L.; Lind, C.; Downie, C.; Vazquez-Alvarez, T.; Angelo, A. C. D.; DiSalvo, F. J.; Abruna, H. D. *J. Am. Chem. Soc.* **2004**, *126*, 4043−4049.
(3) Xiong, L.; Kannan, A. M.; Manthiram, A. *Electrochem. Commun.* **2002**, *4*, 898−903.
(4) Carmo, M.; Paganin, V. A.; Rosolen, J. M.; Gonzalez, E. R. *J. Power Sources* **2005**, *142*, 169−176.
(5) Matsumoto, T.; Komatsu, T.; Arai, K.; Yamazaki, T.; Kijima, M.; Shimizu, H.; Takasawa, Y.; Nakamura, J. *Chem. Commun.* **2004**, 840−841.
(6) Holmes, J. D.; Lyons, D. M.; Ziegler, K. J. *Chem.−Eur. J.* **2003**, *9*, 2144−2150.
(7) Zhang, Y.; Erkey, C. *J. Supercrit. Fluids* **2006**, *38*, 252−267.
(8) Ye, X.-R.; Lin, Y.; Wang, C.; Engelhard, M. H.; Wang, Y.; Wai, C. M. *J. Mater. Chem.* **2004**, *14*, 908−913.
(9) Dhepe, P. L.; Fukuoka, A.; Ichikawa, M. *Phys. Chem. Chem. Phys.* **2003**, *5*, 5565−5573.
(10) Kameo, A.; Yoshimura, T.; Esumi, K. *Colloids Surf., A* **2003**, *215*, 181−189.
(11) Wakayama, H.; Fukushima, Y. *Ind. Eng. Chem. Res.* **2006**, *45*, 3328−3331.

10.1021/ef0606409 CCC: $37.00
Published on Web 05/26/2007

methanol.[12−14] In this paper, a new Pt−Ru sample and several other platinum-based bimetallic catalysts are described for potential DMFC applications.

2. Experimental Section

2.1. Chemicals. MWCNT (Nanostructured and Amorphous Materials, Inc.; Houston, TX) were treated and functionalized according to a previous study.[5] Several CO_2-soluble metal precursors including platinum(II) acetylacetonate [$Pt(acac)_2$, Aldrich], ruthenium(III) acetylacetonate [$Ru(acac)_3$, Aldrich], nickel(II) hexafluoroacetylacetonate [$Ni(hfa)_2$, Aldrich], palladium(II) hexafluoroacetylacetonate [$Pd(hfa)_2$, Aldrich], copper(II) hexafluoroacetylacetonate [$Cu(hfa)_2$, Alfa Aesar], and gold(III) dimethylacetylacetonate [$AuMe_2(acac)$, Strem Chemicals, Inc., Newburyport, MA] were used as received. High-purity nitrogen (99.97%) was obtained from Oxarc (Spokane, WA). Methanol was obtained from J.T. Baker (HPLC grade). Sulfuric acid was purchased from EMD (ACS grade, Darmstadt, Germany) and titrated against tris(hydroxymethyl)aminomethane (Aldrich) to calibrate before use. Deionized water used in the electrochemical analysis was filtered through a graphite cartridge purchased from Barnstead International (D8922, Dubuque, IA). Nafion 117 solution (5 wt %) was purchased from Fluka, and ACS/USP-grade ethanol solution was purchased from Pharmco.

2.2. Synthesis of Catalysts. The experimental setup was the same as described in our previous reports.[8,12−14] In a typical trial, the amount of MWCNT and $Pt(acac)_2$ were fixed at 20 mg each. The amount of the secondary metal precursor was adjusted to have a 1:1 molar ratio to $Pt(acac)_2$. Some of the metal precursors have low solubility in CO_2. To increase the solubility of the precursors, a small amount of methanol (∼1 mL) could be added as a modifier to modify the polarity of the CO_2. The metal precursors and the MWCNTs were placed in a high-pressure reaction cell (∼10 mL volume, cylindrical cell with filters on both ends), and 100 atm of CO_2 was added into the cell to dissolve the metal precursors for 1 h. Finding a suitable temperature for both dissolution and reduction of the bimetals is very important. On the basis of optimization of Pt nanoparticle formation, we found 200 °C to be suitable for the formation of Pt-based bimetallic nanoparticles, except for Pt−Au, which should be lowered to 70 °C. After 1 h, a mixture of hydrogen (10 atm) and CO_2 (240 atm) was injected into the cell, which combined to a final pressure of 250 atm. This amount of hydrogen was 10 times in excess for the reduction of the metal precursors based on a stoichiometric calculation. The final pressure was higher than the one used in our previous studies for synthesizing monometallic Pt nanoparticles.[12,13] The choice of the final pressure was based on other reports that a higher pressure could result in a smaller size of the nanoparticles, and we found that 250 atm gave good results for synthesizing bimetallic nanoparticles.[15,16] After 30 min of reduction, the cell was depressurized and cooled down to room temperature. The remaining product inside the cell was then collected and washed several times using methanol with sonication for 10 min each time. It should be noted that ethanol can also be used for the washing process.

2.3. Electrode Modification and Electrochemical Analysis. A 5% Nafion solution was dilluted to 0.5% in a water/ethanol solution (1:1 vol ratio), and a bimetallic nanocatalyst was added to the solution to make a 1 mg/mL catalyst/Nafion mixture. The mixture was sonicated in an ice-water bath for 0.5 h to ensure that the catalyst was evenly dispersed in the mixture. A total of 6 μL of the mixture was pipetted onto the surface of a clean glassy carbon electrode (GC, 3 mm in diameter, BAS, West Lafayette, IN) and air-dried for 2 h at ambient temperature. The modified electrode was then placed in deoxygenated 1 M H_2SO_4 to obtain a background current for up to 40 scans. This process helped stabilize the cyclic voltammogram (CV) of methanol oxidation. The CV was conducted using a conventional three-electrode cell, consisting of an Ag/AgCl reference electrode (saturated KCl, BAS), a carbon rod auxiliary electrode (99%, Alfa Aesar), and the modified working electrode. Potentials are corrected to the normal hydrogen reference electrode (NHE) for the reporting purpose. Pure methanol and the stock solution of sulfuric acid as well as deionized water were purged with nitrogen separately for 1 h to remove the dissolved oxygen. Methanol and DI water were purged with dry nitrogen; however, nitrogen has to purge sulfuric acid through the DI water bomb to keep the concentration constant. The degassed solutions were mixed in the reaction cell to make a mixture of 2 M methanol and 1 M sulfuric acid right before CV was conducted. CV was scanned from 100 to 900 mV versus Ag/AgCl at 60 mV/s.

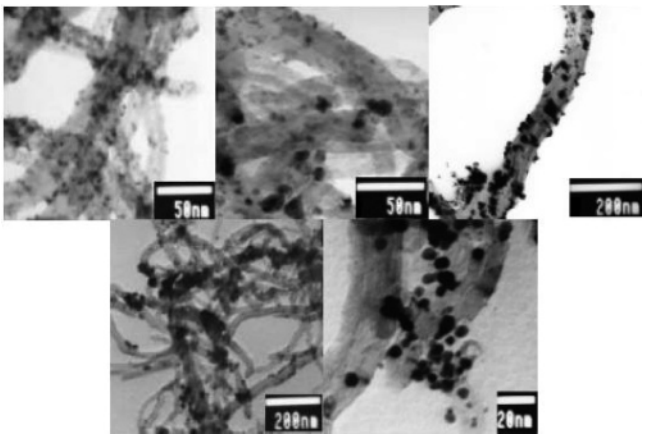

Figure 1. TEM of (a) Pt−Ru (top left), (b) Pt−Ni (top middle), (c) Pt−Au (top right), (d) Pt−Pd (bottom left), and (e) Pt−Cu (bottom right).

3. Results and Discussion

3.1. Characterization of Catalysts. Figure 1 shows the transmission electron microscopy (TEM; Joel JEM-1200EXII) images for each pair of the bimetallic nanoparticles deposited on the MWCNTs. The TEM pictures of the bimetallic nanoparticles did not show observable differences between the washed and unwashed materials. The average sizes of the bimetallic nanoparticles on the MWCNTs are different depending upon the metal pairs and were calculated using an interactive imaging software from Matrox Electronic Systems. A minimum of 100 nanoparticles were counted, and the average size and standard deviation are listed in Table 1.

X-ray diffraction (XRD) patterns were obtained using a Siemens D5000. The broad peak between 25° and 30° can be assigned to MWCNT, which has a graphite-like structure. In all cases, except in Pt−Ru, the diffraction patterns showed face-centered cubic (fcc) structures. The (111) peaks of each kind of bimetallic nanoparticles are all located between the peaks of pure Pt (111) ($2\theta = 39.8°$) and the pure secondary metal (111): Au ($2\theta = 38.2°$), Pd ($2\theta = 40.1°$), Cu ($2\theta = 43.3°$), and Ni ($2\theta = 44.5°$). The situation is also true for the (200) peaks of the bimetallic nanoparticles, which are all located between the (200) peaks of the pure Pt ($2\theta = 46.2°$) and the pure secondary metal: Au ($2\theta = 44.4°$), Pd ($2\theta = 46.7°$), Cu ($2\theta = 50.4°$), and Ni ($2\theta = 51.8°$). These results may suggest

(12) Lin, Y.; Cui, X.; Yen, C.; Wai, C. M. *J. Phys. Chem. B* **2005**, *109*, 14410−14415.
(13) Yen, C. H.; Cui, X.; Pan, H.-B.; Wang, S.; Lin, Y.; Wai, C. M. *J. Nanosci. Nanotechnol.* **2005**, *5*, 1852−1857.
(14) Lin, Y.; Cui, X.; Yen, C. H.; Wai, C. M. *Langmuir* **2005**, *21*, 11474−11479.
(15) Shah, P. S.; Husain, S.; Johnston, K. P.; Korgel, B. A. *J. Phys. Chem. B* **2002**, *106*, 12178−12185.
(16) Chatterjee, M.; Ikushima, Y.; Hakuta, Y.; Kawanami, H. *Adv. Synth. Catal.* **2006**, *348*, 1580−1590.

Table 1. Conditions and Results of Chemical Fluid Deposition[a]

	metal precursors	T (°C)	particle size (nm)
Pt−Ru	$Pt(acac)_2$ $Ru(acac)_3$	200	2.8 ± 0.8
Pt−Ni	$Pt(acac)_2$ $Ni(hfa)_2$	200	6.6 ± 3.5
Pt−Au	$Pt(acac)_2$ $(CH_3)_2(acac)Au$	70	9.3 ± 3.7
Pt−Pd	$Pt(acac)_2$ $Pd(hfa)_2$	200	9.2 ± 3.3
Pt−Cu	$Pt(acac)_2$ $Cu(hfa)_2$	200	5.7 ± 2.2

[a] The condition for dissolution is 100 atm of CO_2 for 1 h. The condition for reduction is 10 atm of H_2 plus 240 atm of CO_2 for 30 min.

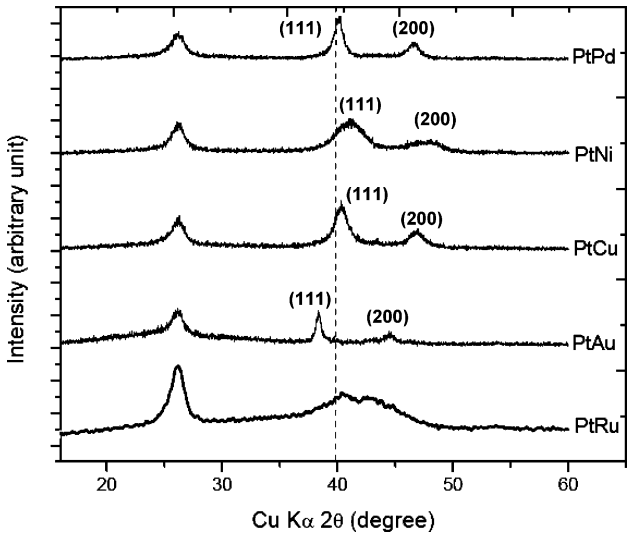

Figure 2. XRD patterns of the different bimetallic catalysts. The dotted line is the monometallic Pt (111) ($2\theta = 39.8°$) peak for reference.

that the bimetallic nanoparticles have disordered alloy crystal structures.[17−19] In the case of Pt−Ru, because Ru has a hexagonal close-packed (hcp) structure that is different from Pt, the diffraction pattern showed a mixture of both fcc and hcp. Previous reports also suggested that the major metal of the bimetallic nanoparticle would show more predominant characteristics in the diffraction patterns.[20,21] The XRD patterns of the different bimetallic nanoparticles are provided in Figure 2.

Energy-dispersive X-ray spectroscopy (EDS; LEO SUPRA 35VP FESEM) could provide the quantitative analysis of our samples, and the results are shown in Table 2. Interestingly, we found that, even when the amount of the metal precursors were fixed at a 1:1 ratio, only the ratio of the two metals of the Pt−Ru and Pt−Pd bimetallic nanoparticles would still maintain close to unity. In other cases, platinum tends to be the major component in the bimetallic nanoparticles, except in the case of Pt−Au. The temperature (200 °C) for the synthesis appeared suitable for synthesizing fine bimetallic nanoparticles described

Table 2. Results of the Quantitative Analysis by EDS

	Pt wt %	Pt atom %	second metal wt %	second metal atom %	Pt−second metal
Pt−Ru	21.30	1.96	11.77	2.10	48:52
Pt−Ni	23.13	2.00	4.47	1.22	62:38
Pt−Au	4.28	0.30	7.24	0.50	37:63
Pt−Pd	31.77	3.70	17.29	3.74	50:50
Pt−Cu	21.75	1.77	3.68	0.92	66:34

in this paper, and a further increase in the temperature did not seem to affect the particle size, except for the Pt−Au system. Even at 200 °C, large Pt−Au particles (100-200 nm) were observed, which would cause poor electrocatalytic activity according to our experiments. Cabanas et al. also reported that the size of the Au nanocrystals formed in sc-CO_2 at 125 °C was much larger than those formed at 60 °C.[22] For this study, we chose 70 °C as the temperature for Pt−Au synthesis in this study. For the other bimetallic systems, which the temperature was fixed in 200 °C, Pt−Pd has a relatively higher weight and atom percentage compared to others. This is probably due to the special property of Pd called the "electron-mediating effect", which, in this case, can help the reduction of Pt−Pd more completely.[23] A similar situation was also observed in a previous study of making Cu film, in which Pd was added to lower the temperature of the reduction process.[24] Generally, different bimetallic combinations have different kinetics in hydrogen reduction because of their different redox potentials and activation energies.[23] Therefore, we believe this is the main reason that is causing the differences of the compositions in different bimetallic systems. Another reasonable explanation could be due to the washing process, and some of the nanoparticles that are not attached strongly enough to the wall of the MWCNTs may fall off. Therefore, these bimetallic nanoparticles could result in different weight and atom percentages. From the atom percent data obtained from the EDS analysis that is listed in Table 2, we calculated the ratios of the following bimetallic nanoparticles: Pt−Ru (48:52), Pt−Ni (62:38), Pt−Au (37:63), Pt−Pd (50:50), and Pt−Cu (66:34). Further experiments are continuing for this study.

3.2. Electrocatalytic Activities of Catalysts. Electrocatalytic activities of the MWCNT-supported bimetallic nanoparticles for the oxidation of methanol were examined using CV (Figure 3). The voltammograms consist of two oxidation peaks: one in the forward scan (arrow left to right) and the other in the backward scan. It was observed that the oxidation of the platinum and bimetallic surfaces occurred during the forward scan when the switching potential exceeded 1.1 V versus NHE, and during the backward scan, the reduction peak was observed at around 0.7−0.8 V versus NHE. Hence, the CV was conducted within the potential range of 1.1 and 0.3 V versus NHE. As seen in Figure 3, backward scans do not contain the oxidation/reduction peak of platinum or the secondary metals. The forward scan is attributable to methanol oxidation, forming Pt-adsorbed carbonaceous intermediates, including carbon monoxide (reaction 1) and CO_2 (reaction 2). This adsorbed carbon

(17) Xiong, L.; Manthiram, A. *J. Electrochem. Soc.* **2005**, *152*, A697−A703.
(18) Wu, M.-L.; Chen, D.-H.; Huang, T.-C. *Chem. Mater.* **2001**, *13*, 599−606.
(19) Wu, M.-L.; Chen, D.-H.; Huang, T.-C. *J. Colloid Interface Sci.* **2001**, *243*, 102−108.
(20) Liu, Z.; Ling, X. Y.; Su, X.; Lee, J. Y. *J. Phys. Chem. B* **2004**, *108*, 8234−8240.
(21) Chu, D.; Gilman, S. *J. Electrochem. Soc.* **1996**, *143*, 1685−1690.
(22) Cabanas, A.; Long, D. P.; Watkins, J. J. *Chem. Mater.* **2004**, *16*, 2028−2033.
(23) Yonezawa, T.; Toshima, N. *J. Chem. Soc., Faraday Trans.* **1995**, *91*, 4111−4119.
(24) Ohde, H.; Kramer, S.; Moore, S.; Wai, C. M. *Chem. Mater.* **2004**, *16*, 4028−4031.

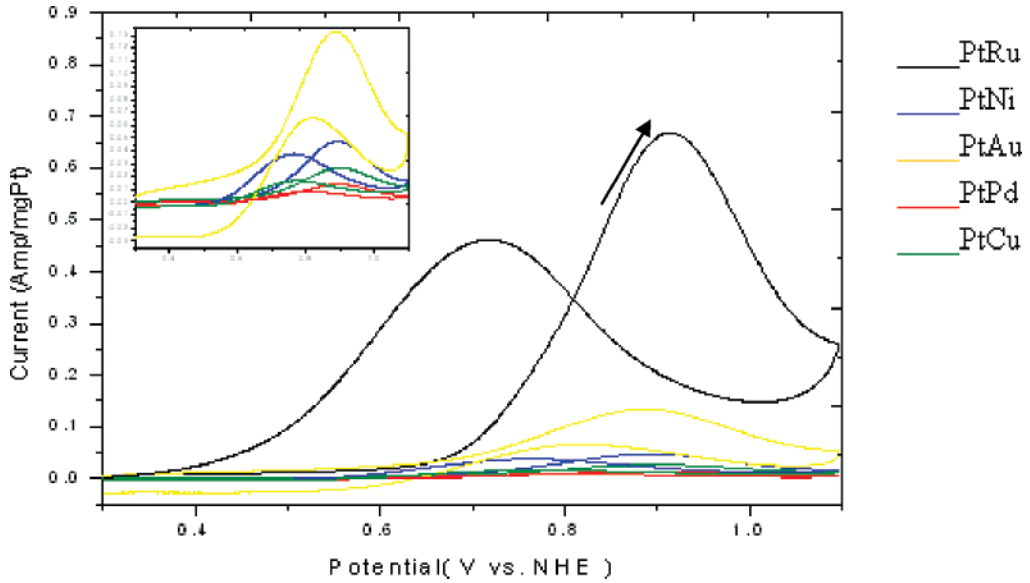

Figure 3. Typical cyclic voltammograms of the methanol oxidation with different bimetallic nanoparticle catalysts in 2 M CH_3OH and 1 M H_2SO_4 under deoxygenated conditions. The scan rate was 60 mV/s, and the scan direction is shown with an arrow.

monoxide (CO_{ads}) causes the loss of activity of the electrocatalyst.[20,25,26]

$$Pt + CH_3OH \rightarrow Pt{-}CO_{ads} + 4H^+ + 4e^- \quad (1)$$

$$CH_3OH + H_2O \rightarrow CO_2 + 6H^+ + 6e^- \quad (2)$$

$$(E^0 = 0.04 \text{ V versus NHE})$$

The backward oxidation peak, shown as reaction 3, is attributed to the additional oxidation of the adsorbed carbonaceous species to carbon dioxide.[26]

$$Pt{-}CO_{ads} + H_2O \rightarrow Pt + CO_2 + 2H^+ + 2e^- \quad (3)$$

Therefore, the current ratio of the forward scan peak current (I_f) over the backward scan peak current (I_b) shows the amount of methanol oxidized to carbon dioxide relative to carbon monoxide.[12−14,20,25] A higher I_f/I_b value suggests that the catalysts are more efficient at lowering the adsorbed carbon monoxide. The current ratio is a useful way of comparing the long-term catalytic activity between the different catalysts. Previous investigators have conducted a chronoamperometric along with a CV studies and demonstrated that catalysts with a higher I_f/I_b ratio are correlated with catalyst longevity.[12−14,20,25,28] The MWCNT-supported bimetallic nanoparticle catalysts all exhibit at least 60% higher I_f/I_b ratios relative to that of Pt monometallic nanoparticles ($I_f/I_b = 1.4$), which is also prepared by the CFD method. It is interesting to note that the Pt−Au bimetallic system has a high I_f/I_b ratio (2.50) next to that of the Pt−Ru system (2.95). The other three bimetallic systems, Pt−Pd, Pt−Ni, and Pt−Cu all have I_f/I_b ratios about 2.3, which are lower than that of the Pt−Au bimetallic system. Table 3 summarizes the onset potentials, the forward peak potentials, the forward peak current, and the current ratios (I_f/I_b) of each bimetallic electrocatalyst. The onset potential suggests the apparent activation energy of methanol oxidation and of the Pt−Ru catalyst is 411 mV versus NHE, which is in good agreement with reported values for the Pt−Ru catalyst with a similar atomic ratio.[20,25,29,30] All of the Pt-based bimetallic catalysts have a lower onset potential than that of the Pt monometallic catalyst, with the onset potential of Pt−Pd being the lowest.

Table 3. Comparison of the Electrochemical Activities of the Catalysts

	onset potential (mV versus NHE)	forward peak potential (mV versus NHE)	forward peak current (A/mg of Pt)	I_f/I_b current ratio (efficiency)
Pt[12]	446	886	0.096	1.42
Pt−Ru	411	913	0.68	2.95
Pt−Ni	409	892	0.052	2.34
Pt−Au	431	887	0.10	2.50
Pt−Pd	351	898	0.033	2.35
Pt−Cu	424	899	0.031	2.31

4. Conclusion

In conclusion, the CFD method of making MWCNT-supported bimetallic nanoparticles appears to provide a simple way of preparing and studying catalytic properties of various bimetallic nanocatalysts. These new nanocatalysts are not only important for the development of more efficient PEMFCs, but also the technology itself represents a green chemistry approach for nanomaterial synthesis. Furthermore, the performances of these Pt-based bimetallic catalysts are better or at least comparable to literature systems and also show improvements compared to the Pt monometallic catalyst.

Acknowledgment. This work was supported by the Electric Power Research Institute (EP-P18031/C8893) and the Air Force Office of Scientific Research (F49620-03-1-0361). Support of the S. T. Li Foundation for the Award for Achievements in Science and Technology (to C.M.W.) is acknowledged.

EF0606409

(25) Huang, J.; Liu, Z.; He, C.; Gan, L. M. *J. Phys. Chem. B* **2005**, *109*, 16644−16649.
(26) Hoogers, G. *Fuel Cell Technology Handbook*; CRC Press: Boca Raton, FL, 2003.
(27) Manoharan, R.; Goodenough, J. B. *J. Mater. Chem.* **1992**, *2*, 875−887.
(28) Iwasita, T.; Hoster, H.; John-Anacker, A.; Lin, W. F.; Vielstich, W. *Langmuir* **2000**, *16*, 522−529.
(29) Page, T.; Johnson, R.; Hormes, J.; Noding, S.; Rambabu, B. *J. Electroanal. Chem.* **2000**, *485*, 34−41.
(30) Prabhuram, J.; Zhao, T. S.; Tang, Z. K.; Chen, R.; Liang, Z. X. *J. Phys. Chem. B* **2006**, *110*, 5245−5252.